J. Rubb. Res., **21(3)**, 165-181

Effect of Simultaneous Use of Silica and Nanoclay in Rubber Compounds Based on Nitrile Rubber

M.M. SALEHI[1#], T. KHALKHALI[1] AND A.R. DOURBASH[1]

The synergistic effect of simultaneous use of two reinforcing fillers in rubber compounds based on Acrylonitrile Butadiene Rubber (NBR) was investigated with mechanical and vulcanisation characteristics of the rubber compounds. The Wide-Angle X-ray Diffraction (WAXD) patterns showed that in hybrid compounds, no obvious peaks appeared. This indicated that the nanoclay was exfoliated. These results revealed that addition of the reinforcing filler, either nanoclay or silica, shortened the optimum cure time (t_{90}) and also scorch time (t_{s1}) of samples compared to that of pure NBR compound. In hybrid compounds, the reduction in optimum cure time and scorch time was higher than that of for silica-filled NBR or nanoclay-filled NBR compounds. This can be attributed to the synergistic effect between nanoclay and silica as two reinforcing agents in NBR compounds. Regardless the composition of the reinforcing filler, an increase of the relaxed storage modulus was observed, while the tanδ value was gradually decreased. For hybrid samples, the experimental values of dynamic modulus showed a positive deviation from the values obtained from the Modified Guth model. Hybrid compounds showed higher burst strength compared to silica or nanoclay filled NBR compounds.

Keywords: Silica; nanoclay; NBR; mechanical properties; synergistic effect

Many industries, such as petrochemical, chemical, pharmaceutical, food processing, and oilfield applications, rely on pressurised equipment and assemblies such as pressure vessels and propellant subsystems. Burst diaphragms, also referred to as bursting discs and rupture discs, as pressure relief devices, sacrificially protect mission-critical systems from predetermined differential pressure, either positive or negative, that is, over pressurisation and potentially damaging vacuum conditions. Major advantages of the use of rupture discs compared to pressure relief valves would be leak tightness, no maintenance and cost. Burst discs usually have steel or aluminum housings enveloping a one-time-use membrane commonly made of cold-rolled steel, nickel alloys, aluminum, or any other material with yield strength close to its ultimate strength. Nitrile rubber and hydrogenated Nitrile Butadiene Rubber, as a family of unsaturated copolymers of acrylonitrile (ACN), are commonly used to produce such diaphragms operating up to 120 °C. Acrylonitrile Butadiene Rubber (NBR) is resistant to aliphatic hydrocarbons, oil, and fuel and hence is selected for this study contemplated for oilfield applications[1]. However, the mechanical properties, ozone resistance and processability of NBR are poor[2]. Fillers such as silica, carbon black, layered silicates, and carbon nanotubes are usually added to improve its physical and mechanical strength[3-12]. The choice of the elastomer compound additives is closely linked to the type of properties to be achieved.

[1] Formulation and Development of Applications of Chemical and Polymeric Compounds Research Group, Chemical, Polymeric and Petrochemical Technology Development Research Division, Research Institute of Petroleum Industry, Tehran, Iran.

[#] Corresponding author (e-mail:salehimm@ripi.ir)

The property improvement of nanocomposites depend on several factors including the size of the particles, their aspect ratio, their degree of dispersion and orientation in the matrix and the strength of interactions between the filler and the matrix polymer[3]. However, the addition of fillers has some limitations and desired properties cannot be achieved. The idea of combination of fillers in order to make use of synergistic effects which can be used as a convenient method to improve the properties of elastomeric compounds is discussed[1, 3-5, 8, 11, 13]. In this regards, Bendahou *et al*.[13], investigated the synergistic effect of nanoclay and cellulose whiskers on the mechanical and barrier properties of natural rubber (NR) composites. They found that the nanoclay dispersion state was totally modified as cellulose whiskers were introduced in the matrix. The calculated tortuosity values indicated that the simultaneous use of nanoclay and whiskers could greatly slow down the gas diffusion rate in NR. Formation of nanoclay-whiskers subassembly should be responsible for this synergistic effect. Chen *et al*.[2], investigated the thermal degradation behavior of hydrogenated nitrile-butadiene rubber (HNBR) with clay and carbon nanotubes (CNT). They showed that the HNBR/clay/CNTs nanocomposites had lower thermal degradation rate than HNBR/clay, which could be attributed to that the clay-CNTs filler network reduced the diffusion speed of degradation products. The coexistence of clay and CNTs could form compact char layers with better barrier properties than clay and thus improved the thermal stability of HNBR. Praveen *et al*.[5], evaluated the structure-properties of SBR/nanoclay/carbon black (CB) hybrid nanocomposites. Tensile results of CB filled SBR nanocomposites showed remarkable improvement in strength properties. This suggests there was a synergistic interaction between CB and nanoclay. Salkhord *et al*.[14], investigated synergistic reinforcement of NBR by hybrid filler system including organoclay and nano-$CaCO_3$. They found that synchronous use of nanofillers to NBR leads to better dispersion of nanofillers because the collisions and friction of nanoparticles and nanolayers, so leading to breakdown of filler agglomerates.

Except carbon black, silica is one of the most important filler used in the NBR compound[11, 15]. Nitrile rubber exhibited the highest interaction with silica probably through the hydrogen bond between the –CN group and silanol groups[15]. In addition, silica (SiO_2) as reinforcing filler has been preferentially selected for preparing vulcanisates with a unique combination of tear strength, abrasion resistance, age resistance, and adhesion properties[3, 15].

To our best knowledge, there is no report on the use of combination of silica with organomodified clay for improving the physical and mechanical properties of NBR compounds. In this regards, we investigated the synergistic effect of silica with organoclay on the physical, mechanical and curing properties of NBR compounds.

EXPERIMENTAL

Materials

The following materials were employed in this work reported here.

Rubber:
Acrylonitrile-butadiene rubber (NBR) with 45 wt% acrylonitrile (ACN) (Mooney viscosity, ML1+4, at 100 °C = 60) was provided by Polimeri Europa Co., Ltd.

Fillers:
1) The precipitated silica (VN3) powder with a surface area 175 m^2/g comes from Evonik Degussa, Germany.

2) Organosilicate intercalated by dimethyl, dehydrogenated tallow, and quaternary ammonium (Cloisite 15A, Southern Clay Products Inc.) with aspect ratio 75:100 was used in this work.

Accelerators:
1) N-cyclohexyl-2-benzothiazole sulphenamide (CBS), melting point 95-100 °C and specific gravity 1.27-1.31 g.cm^{-3}.
2) Tetramethylthiuram Disulfide (TMTD), melting point 156-158 °C and specific gravity 1.43 g.cm^{-3}. These accelerators were supplied by Shenzhen Sendi Biotechnology Co.Ltd.

Antioxidants:
N-isopropyl-N'-phenyl-p-phenylenediamine (IPPD-4010), melting point 70 °C and specific gravity 1.26-1.32 g.cm^{-3}. IPPD-4010 was provided by Hebi Hifull Trade Co. Ltd.

Curing Agent:
Sulfur, purity 99.9%, melting point 112 °C and specific gravity 2.04-2.06 g.cm^{-3}. The curing agent was purchased from Maron Rubber Co. Ltd (Iran).

Activator:
1) Zinc oxide (ZnO) with purity 99%, specific gravity 5.6 g.cm^{-3}.
2) Stearic acid with melting point 67-69 °C, specific gravity 0.838 g.cm^{-3}. The activators were purchased from Maron Rubber Co. Ltd (Iran).

Processing aid: Dioctyl phthalate (DOP), boiling point 384 °C and specific gravity 0.986 g.cm^{-3}. DOP was supplied by Maron Rubber Co. Ltd (Iran).

Sample Preparation

All the samples were prepared by melt compounding on a two-roll mill with a friction ratio of 1:1.4 at 50 ˚C. The denoted codes and composition of the samples are described in *Table 1*. NBR was masticated for 3 min and the other ingredients were added (*Table 1*). Polymer (NBR), filler (silica, Cloisite 15A), antioxidants and processing aid (IPPD, DOP), activators (ZnO, Stearic acid), vulcanisation aids (TMTD, CBS and sulfur) were added respectively and mixed during compounding. The processing time after each component

TABLE 1. FORMULATION OF NBR COMPOUNDS

Ingredients *	NBR0:0	NBR25:0	NBR0:3	NBR0:5	NBR25:3	NBR25:5
NBR	100	100	100	100	100	100
Silica	0	25	0	0	25	25
Cloisite 15A	0	0	3	5	3	5
DOP	15	15	15	15	15	15
IPPD	1.5	1.5	1.5	1.5	1.5	1.5
ZnO	5	5	5	5	5	5
ST.A.	1	1	1	1	1	1
TMTD	1.5	1.5	1.5	1.5	1.5	1.5
CBS	1.5	1.5	1.5	1.5	1.5	1.5
Sulphur	1.5	1.5	1.5	1.5	1.5	1.5

* Amount indicated here is in parts per hundred gram rubber (phr) basis.

addition was about 2 min. The compound rubber was allowed to stand overnight before vulcanisation in order to release the remaining stress of rubber chains after the mixing process. Vulcanisation characteristics of the samples were determined using a Monsanto Oscillating Disk Rheometer 100 at 150 ˚C. Then, the rubber compounds molded in the form of sheets (width 15 × 15 cm, thickness 2 mm) in an electrically heated hydraulic press at their optimum cures obtained from rheometer at 150˚ C.

Sample Characterisation

Cure properties of the rubber compounds. The scorch time (t_{s1}), which is the time for the onset of cure, and the optimum cure time (t_{90}), which is the time for the completion of cure, were determined using a Monsanto Oscillating Disk Rheometer 100 at 150 ˚C. ΔM, which is the difference between the maximum and minimum torque values on the cure trace of the rubber. The cure rate index (CRI), which is a measure of the rate of curing in the rubber, was calculated using,

$$CRI = 100 / (t_{90} - t_{s1}) \quad \ldots 1$$

WAXD measurements. WAXD experiments were conducted on the samples using a Phillips X'pert diffractometer with Cu-Kα radiation of wavelength (λ) 0.154 nm generated at 40 kV and 40 mA. The diffractograms were scanned in the 2θ range from 1° to 10° at the rate of 1°/min at ambient temperature (23±2 °C) and the measurements were recorded every 0.04°.

Microstructure characterisation. The filler dispersion state was observed at different scales using a scanning electron microscope, SEM, (Hitachi 4160, Japan) with 20 kV accelerating voltage. The cryogenically fractured surfaces were coated with gold for enhanced conductivity using SPI sputter coater. A TEM, Philips EM 208 operating at 100 kV, was used to study the state of nanoclay dispersion in the samples. The TEM samples were prepared by using cryo-microtoming at -80 °C to prevent any possible morphological changes during cutting.

Mechanical properties. Tensile specimens were punched out from the molded sheets using ASTM Die-C. The tests were carried out as per the ASTM D 412 methods[16] in a Gotech Testing Machines Inc. (Gotech/GT-7016-A, Taiwan) at a cross head speed of 500 mm/min. Results were averaged on five measurements. IRHD hardness was measured with a Zwick hardness tester according to the standard ASTM D2240[17]. A set up was developed in our laboratory to measure burst performance of diaphragm samples. This is equipped to a chamber (with maximum allowable pressure of 50 bar) lid with two flanges, hydraulic test pump, and transducer (*Figure 1*). A pressure gauge was devised to monitor the pressure variations with time. The internal pressure in chamber increases with hydraulic pump and when the diaphragm ruptures, the burst pressure is determined.

Dynamic mechanical thermal analysis (DMTA). The dynamic mechanical thermal analyses tests were conducted using rectangular samples having dimensions of 25 mm × 10 mm × 2 mm on DMTA machine, Triton-Tritec 2000, United Kingdom in the single cantilever bending mode as per ASTM E1640[18]. The dynamic temperature sweep tests were conducted at 1 Hz frequency and 0.05% strain within temperature ranges of -100 to +100 °C at a heating rate of 5 °C/min.

RESULTS AND DISCUSSION

Microstructure Characterisation

Figure 2 shows the WAXD patterns of organically modified montmorillonite (Cloisite 15A) and several NBR hybrid nanocomposites.

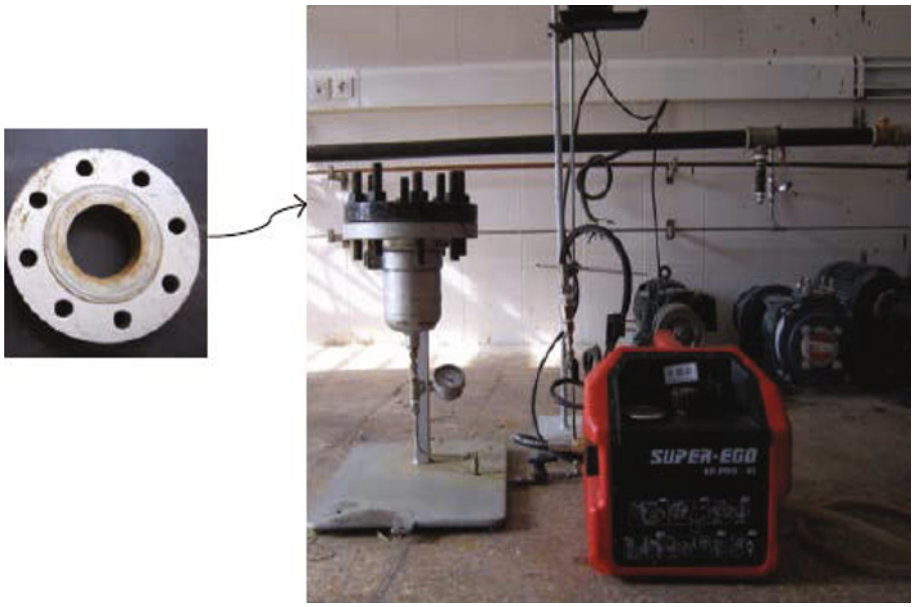

Figure 1. Burst strength measurement set up designed for characterising diaphragm samples.

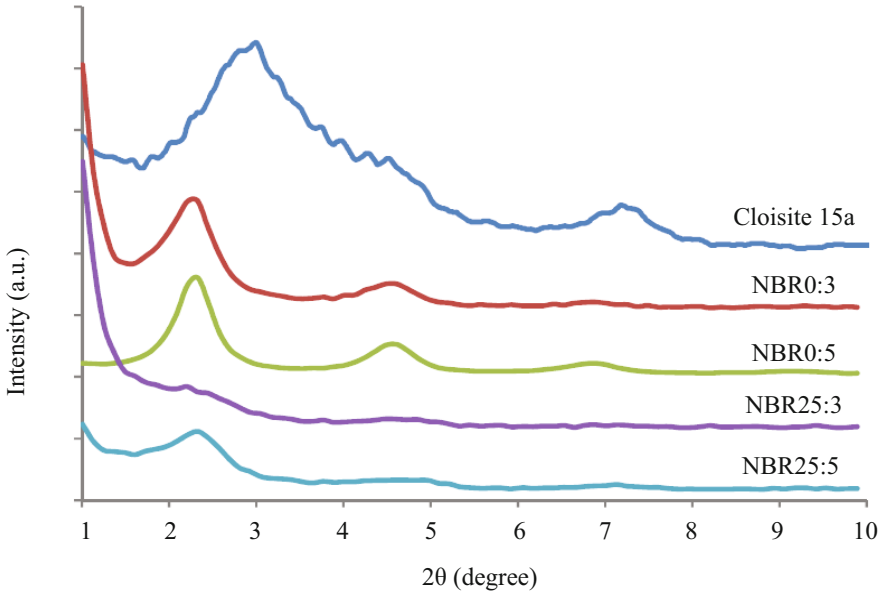

Figure 2. XRD patterns for the Cloisite 15A and NBR hybrid nanocomposites.

The organoclay had two characteristic peaks at 2θ = 2.97° and 7.18°. The interlayer spacings, calculated based on the Bragg formula, are given in *Table 2*. The characteristic peaks of the organoclay were changed for the hybrid samples. The presence of higher order peaks (peak 2 in *Table 2*) confirmed the presence of ordered tactoids in the nanocomposites. The extent of intercalation was almost equal for clay-filled compounds (NBR0:3 and NBR0:5) which indicated that NBR had a fixed ability to make the intercalation structure of Cloisite 15A.

However, in hybrid compound (NBR25:3), no obvious peaks appeared. This indicates that the Cloisite 15A is exfoliated or at least intercalated with an interspacing larger than 88 A°, which cannot be detected with XRD[19]. Achieving to this microstructure could possibly be obtained by the higher mechanical stresses imposed on the NBR matrix with higher viscosity (due to the presence of 25 phr silica) during the mixing on the two roll mill, forcing the separation of the clay lamellae.

When the Cloisite 15A was further increased in hybrid compounds (NBR25:5), a peak was observed at 2θ = 2.21° (d = 39.9 A°), indicating the existence of stacked organolayers of crystallographic order in the NBR matrix. It could be explained by considering the intercalation structure of organoclays. The silica filled compound (NBR25:0) show no reflections 2θ < 10° as being amorphous.

The morphological analysis of the nanocomposites was done using equipments such as TEM and SEM. The transmission electron microscopy (TEM), which provides clear evidence for the delamination of organoclay in NBR matrix. *Figure 3* shows the TEM micrographs for hybrid NBR compounds. Silica particles appear as bright entities whereas organoclays appear as dark lines. Due to the good affinity between the silica and NBR chains, silica can be dispersed well in NBR matrix. Also, most of the organoclay platelets are well dispersed in the NBR matrix, and intercalated microstructure formed in hybrid compounds. These results are consistent with the results obtained in WAXD patterns.

The dispersion of silica and organoclay in NBR matrix and their interaction with together in presence of NBR can be obtained by the SEM micrographs as shown in *Figure 4*.

Silica aggregates are visible as small white spots on the background. These micrographs show good dispersion and distribution of silica and organoclay. It may be due to the good affinity between the reinforcing fillers with NBR matrix[20].

TABLE 2. THE INTERLAYER SPACING VALUES CORRESPONDING TO THE WAXD PATTERNS SHOWN IN FIGURE 2

Sample	Peak 1 2θ (°), **d-spacing (A°)**	Peak 2 2θ (°), **d-spacing (A°)**
Cloisite 15A	2.97, **29.7**	7.18, **12.3**
NBR0:3	2.33, **37.9**	4.61, **19.2**
NBR0:5	2.30, **38.4**	4.55, **19.4**
NBR25:3	-	-
NBR25:5	2.21, **39.9**	-

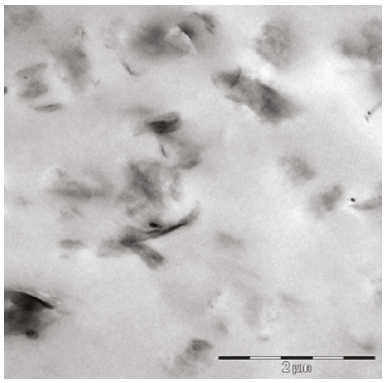

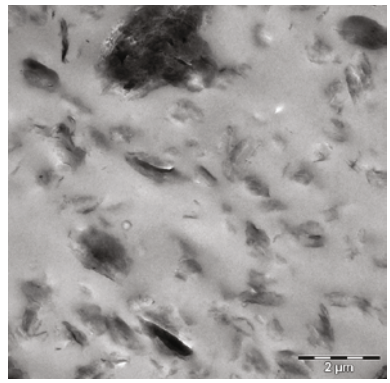

NBR25:3 NBR25:5

Figure 3. TEM micrographs of hybrid NBR compounds.

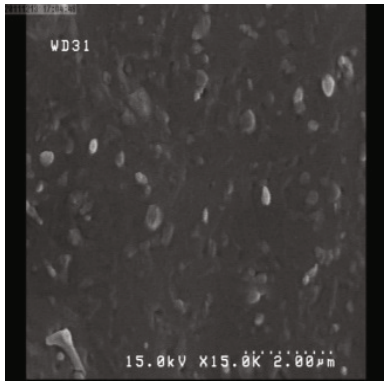

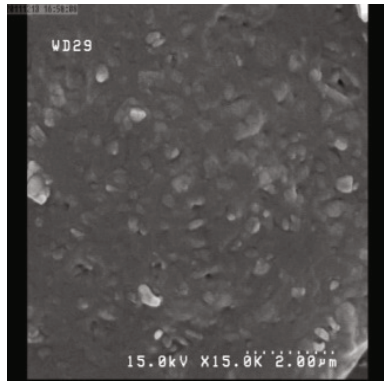

NBR0:3 NBR0:5

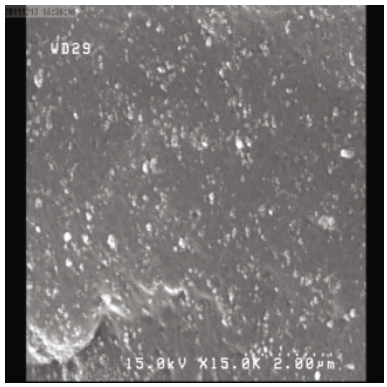

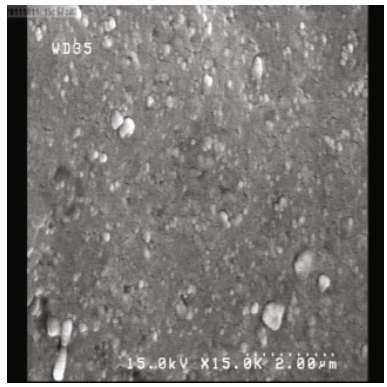

NBR25:3 NBR25:5

Figure 4. Scanning electron microscopy (SEM) observation of NBR compounds.

Curing Characteristics

Vulcanisation graphs of the NBR compounds were shown in *Figure 5*. Corresponding data obtained from the vulcanisation analysis including optimum cure times (t_{90}, t_{s1}), cure rate index and torque values ($\Delta M = M_H - M_L$) are given in *Table 3*.

Comparing the results revealed that addition of the reinforcing filler, either organoclay or silica, shortened the optimum cure time (t_{90}) and also scorch time (t_{s1}) of samples compared to that of pure NBR compound (NBR0:0). On the other hand, the optimum cure time and scorch time both decrease with adding the silica to NBR compounds. This phenomenon can be explained by different mechanisms. In the first mechanism, the reduction was associated with the increase in the compound viscosity and thus the shear heating effect. In the second mechanism, the reduction in cure time can be explained by the increase in effective filler volume by bound rubber for the silica. In fact, NBR chains can be adsorbed on the silica surface, which reduces the volume available for chemicals and thus increases the concentration of the curing agents in the free polymer. This will result in faster onset and higher rate of vulcanization with respect to the neat rubber with no filler. This phenomenon can be correlated to the strength of filler-polymer interaction rather than the chemistry of filler surface which was explained by Wang *et al*.[21].

For the organoclay filled compounds, a reduction in cure time and scorch time compared to the pure NBR compound can be seen. Organoclay behaves like a vulcanising accelerator for NBR matrix. This may be attributed to the complex formation with amines and sulfur containing compounds which facilitates the formation of elemental sulfur[22] and this may be reason for the reduction in scorch and cure time of the organoclay filled compounds.

In hybrid compounds (NBR25:3 and NBR25:5) the reduction in optimum cure

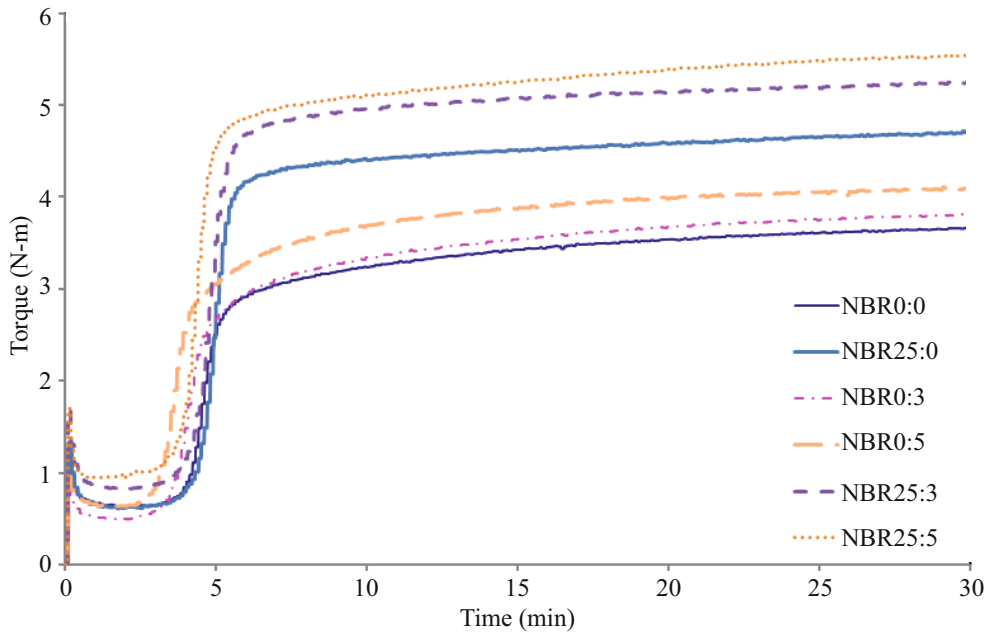

Figure 5. Cure curves of the NBR compounds at 150 ˚C.

TABLE 3. VULCANIZATION CHARACTERISTICS OF THE NBR COMPOUNDS AT 150 ˚C

	NBR0:0	NBR25:0	NBR0:3	NBR0:5	NBR25:3	NBR25:5
MH (N-m)	3.7	4.6	3.8	4.1	5.2	5.5
ML (N-m)	0.6	0.6	0.5	0.6	0.8	0.9
MH-ML (N-m)	3.1	4.0	3.3	3.5	4.4	4.6
t90 (min)	14	6.8	13.1	11.9	6.5	6.2
ts1 (min)	3.7	3.6	3.1	2.9	3.4	3.2
Cure rate Index (min^{-1})	9.7	31.2	10.0	11.1	32.2	33.3

time and scorch time was higher than that of for silica-filled NBR or clay-filled NBR compounds. This can be attributed to the synergistic effect between clay and silica as two reinforcing agents in NBR compounds.

Table 3 also compares the torque differences ($\Delta M = M_H - M_L$) measured for the elastomer compound samples. The rising trend of torque differences with addition of filler to the NBR compound could be ascribed to the compound viscosity corresponding to the interactions established between the rubber matrix and the reinforcement. Results show that, increasing the torque differences for NBR25:0, NBR25:3 and NBR25:5 compounds were higher than that of for NBR0:3 and NBR0:5 compounds. In fact, the strong interactions between NBR functionalities and the silanol groups present at the silica surface might be responsible for this behavior.

Mechanical Properties

Dynamic mechanical thermal analysis (DMTA). The plots of storage modulus and tanδ vs. temperature of NBR and NBR compounds are shown in Figures 6 and 7, respectively. Corresponding data obtained from the DMTA analysis are given in Table 4.

Regardless the composition of the reinforcing filler, an increase of the relaxed storage modulus (E'_{25}) is observed (*Figure 6* and *Table 4*), while the tanδ value (I_α) is decreased steadily. The decreasing tanδ value can be attributed to the strong mutual interaction between NBR and silica and/or nanoclay that decreases the interfacial slide and relaxation. This phenomenon ultimately results in decreasing lag and thereby lowering of tanδ value. The interfacial interaction is strong because of good dispersion of the nanoclay and/or silica particles in NBR, and the clay platelets and/or particles can function as pseudo-crosslinking points, which results in markedly increasing storage modulus of NBR composites containing silica and/or nanoclay[6, 9-11].

After relaxation, due to the higher volume fraction of silica compared to nanoclay in NBR matrix, the storage modulus of silica filled NBR sample (NBR25:0) are higher than that of nanoclay filled NBR samples (NBR0:3 and NBR0:5).

However, for hybrid samples (NBR25:3 and NBR25:5) the strong increase of the storage modulus and decrease of the magnitude of the loss angle (tanδ) are most probably related to synergistic effect of the two filler in NBR matrix. The polymer chains can be adsorbed on the filler surface which reduces the segmental mobility of the polymer chains[23]. These results in formation of a rubber shell having the high modulus near the filler surface. As the polymer chains move a distance from the filler surface, the modulus value gradually decreases, and the value ultimately reaches the same level

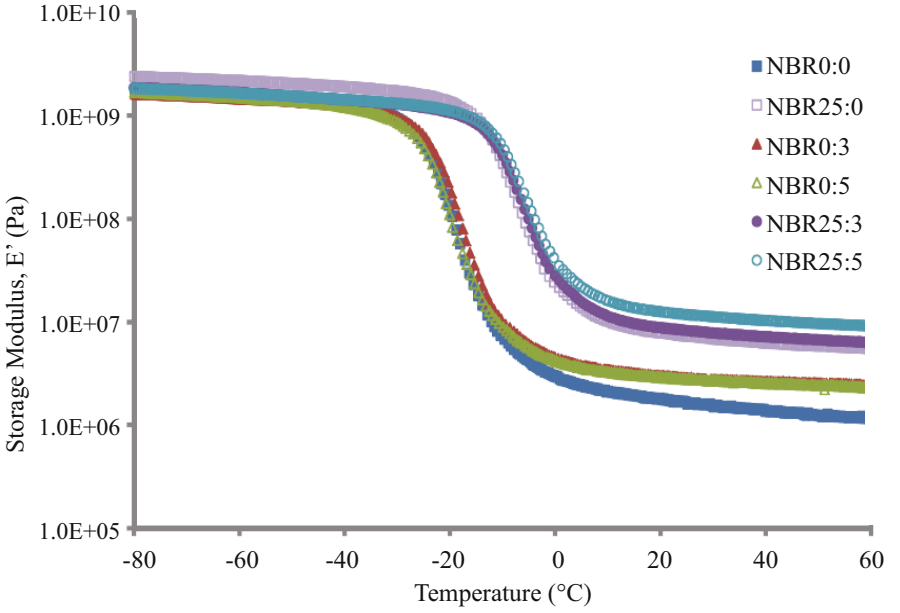

Figure 6. Storage modulus vs. temperature plot of NBR compounds.

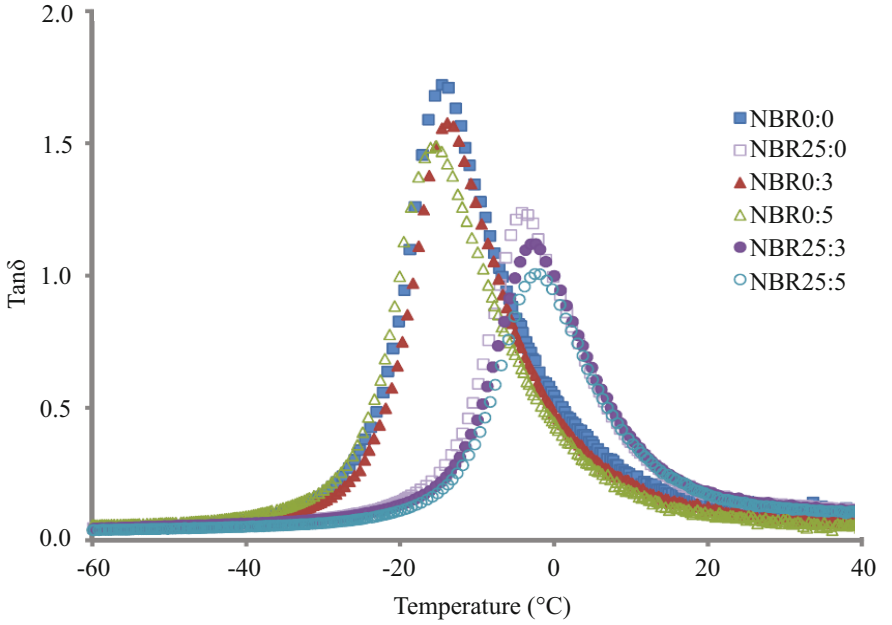

Figure 7. Loss angle (tanδ) vs. temperature plot of NBR compounds.

TABLE 4. RUBBERY STORAGE TENSILE MODULUS E' ESTIMATED AT 25 °C (E'_{25}), AND THE GLASS TRANSITION TEMPERATURE (T_G) AND MAGNITUDE (I_A) OF THE MAIN RELAXATION PROCESS FOR NBR COMPOUNDS

Sample	E'_{25} (MPa)	T_g (°C)	I_α
NBR0:0	1.65	-14	1.72
NBR25:0	7.27	-4	1.23
NBR0:3	2.79	-14.5	1.56
NBR0:5	2.86	-16	1.48
NBR25:3	8.17	-3	1.11
NBR25:5	11.73	-2.5	1.00

as that of the polymer matrix[24]. When two or more aggregates (silica particles and nanoclay platelets) are close enough, they form agglomerate via an adjoining rubber shell where the modulus of the occluded polymer is higher than that of the bulk polymer matrix. The immobilised polymer chains attached to the filler, can lead to an increase in effective volume fraction of the filler in the matrix causing enhancement in dynamic properties such as storage modulus[25]. The same results were observed for nanoclay/carbon black and nanoclay/whiskers hybrid systems[5, 13].

To interpret the variation of the storage modulus of polymeric composites and to predict the reinforcing effect of colloidal fillers on elastomers, the values of the elastic modulus are fitted to the Modified Guth model. Guth[26] introduced a quadratic term on the basis of the Smallwood–Einstein equation to take account of the interaction between filler particles, and obtained the following *Equation 2:*

$$E = E_m[1+2.5\varphi +14.1\varphi^2] \quad \ldots 2$$

where E is Young's modulus of filled elastomer, E_m is matrix Young's modulus, and φ is the volume fraction of filler. *Equation 2* is only applicable to elastomers filled with a certain amount of spherical fillers. If the filler concentration is higher, the modulus increases much more rapidly than the *Equation 2* would predict. The reason can be attributed to the formation of a network involving spherical filler chains. Considering the chains composed of spherical fillers are similar to rod-like filler particles embedded in a continuous matrix, Guth later developed the following *Equation 3* introducing a shape factor, α, in order to account for this 'accelerated stiffening'[27].

$$E = E_m[1+0.67\alpha\varphi +1.62(\alpha\varphi)^2] \quad \ldots 3$$

where E is Young's modulus of filled elastomer, E_m is matrix Young's modulus, φ is the volume fraction of filler, and α is a filler shape factor defined as the ratio between the main and secondary axis of the filler particles[28]. For reinforcing silica particles $\alpha \approx 4$, and for nanoclay $\alpha \approx 15$[29, 30].

Figure 8 shows the comparison of the model predictions with that of experimental values.

It is notable that the values of storage modulus derived from the modified Guth equation matches well with that of experimental values for the silica filled NBR (NBR25:0) and nanoclay filled NBR (NBR0:3 and NBR0:5). However, the values derived from the model have been deviated considerably from the experimental values in case of samples containing hybrid reinforcing

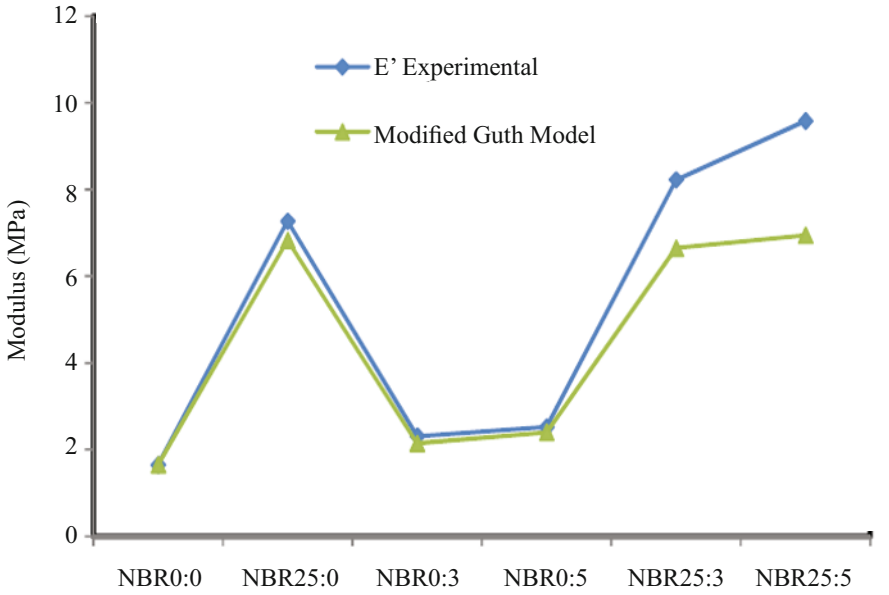

Figure 8. Comparison amongst experimental storage modulus and modified Guth model predicated modulus of NBR compounds.

fillers (NBR25:3 and NBR 25:5). This shows that the model can take into consideration regarding the contribution of nanoclay and/or silica particles.

This discrepancy between experimental and theoretical values of storage modulus in hybrid samples could be explained on the basis silica-nanoclay dual structure formation between silica particles and nanoclay platelets in hybrid samples. Moreover, it can be noticed that the immobilised polymer chains attached to the filler, can lead to an increase in effective volume fraction of the filler in the matrix causing enhancement in dynamic properties such as storage modulus. The Modified Guth model does not take into account the aspect ratio of this structure formed by silica and nanoclay. Therefore, it can be stated that the dual structure and immobilised polymer chains are responsible for the synergistic effect observed in the mechanical and dynamic mechanical properties of hybrid samples.

Tensile Properties

Figure 9 depicts stress-strain behavior for the NBR compounds containing different amounts of silica and nanoclays. As expected, the tensile properties of compounds increases with the addition of reinforcing fillers, either nanoclay or silica. *Table 5* summarises the ultimate properties of tensile strength, elongation at break, stress at 100%, 200% and 300% elongation, and hardness. The mechanical properties of the NBR compounds, such as the tensile strength, elongation at break, stress at different elongation and hardness relative to the pure NBR are enhanced because of the presence of reinforcing fillers.

The tensile strength and stress at 200% elongation for the 25 phr silica filled NBR vulcanisate (NBR25:0) were greater than that for the neat NBR vulcanisate, as expected because of the reinforcement effect and rigidity of silica in the NBR[11]. Loading the silica filler

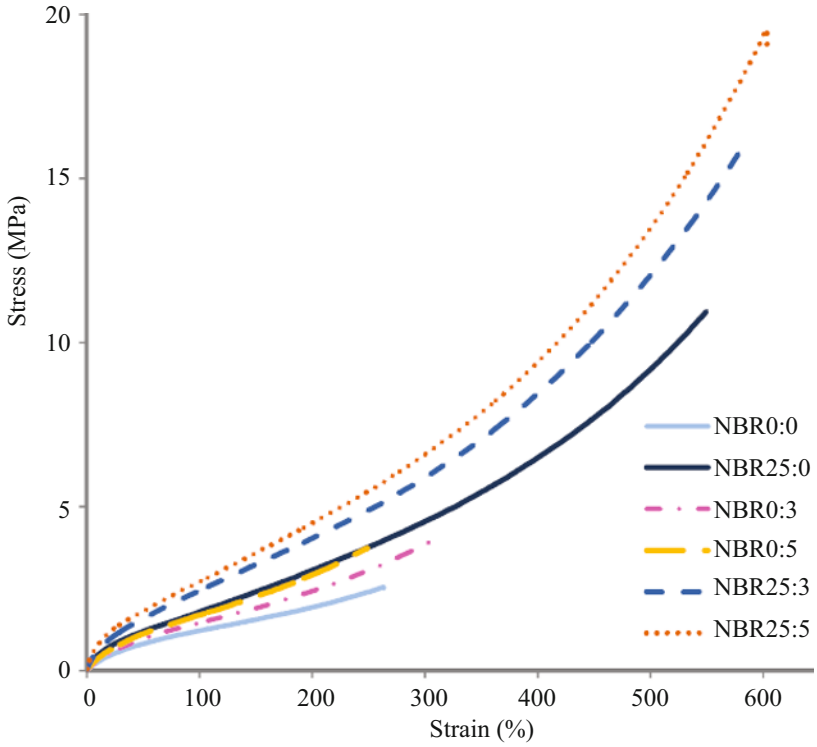

Figure 9. Typical tensile stress/strain curves of the NBR compounds.

TABLE 5. MECHANICAL PROPERTIES OF THE NBR COMPOUNDS

Properties	NBR0:0	NBR25:0	NBR0:3	NBR0:5	NBR25:3	NBR25:5
Hardness (Shore A)	50	58	52	54	62	64
Stress at 100% elongation (MPa)	1.21	1.79	1.46	1.68	2.44	2.70
Stress at 200% elongation (MPa)	1.93	3.06	2.42	2.91	4.03	4.49
Stress at 300% elongation (MPa)	-	4.55	3.84	-	5.88	6.59
Tensile Strength (MPa)	2.54	11.10	3.90	3.73	15.97	19.57
Elongation at Break (%)	263.23	550.09	303.22	248.87	582.07	603.23
Burst Strength (barg), experimental	4.5	7.8	5.1	5.9	11.2	12.5
Burst Strength (barg), calculated from Eq. (5)	3.2	6.7	4.3	5.0	9.2	10.8

resulted in a progressive improvement of the tensile strength of the NBR25:0, the results being in line with the maximum torque results shown in *Figure 5*.

The sample containing 3 phr nanoclay in NBR matrix (NBR0:3) shows a tensile strength of 3.90 MPa and elongation at break of 303%, respectively. It is interesting to note that nanoclay addition has resulted in a steady increase in percent elongation at break and this trend is in-line with the results published in literature for the other nanoclay based rubber-nanocomposites[7, 9]. However, it can be seen from *Figure 9* and *Table 5* that sample containing 25 phr silica (NBR25:0) exhibits the higher tensile strength and elongation at break compared to those of nanoclay filled NBR (NBR0:3 and NBR0:5). This might be due to the high amount and large surface areas of silica providing greater reinforcement.

Surprisingly, NBR samples containing combination of silica and nanoclay (NBR25:3 and NBR25:5) show an increase in strength properties of the composites. Addition of 5 phr nanoclay to the NBR sample containing 25 phr silica shows an increased tensile strength value of 19.57 MPa. This value is exactly 76% compared to the tensile strength value of the NBR25:0. This suggests a synergistic effect between the silica and nanoclay. Moreover, at high strains, strain-hardening behavior is observed for these hybrid samples. The platelets arrangement of nanoclay allows for chain slippage thus preventing the breakage of molecules at higher strains while the bound rubber in silica structure contributes to the modulus and strength. It is important to mention here that the elongations at break for the hybrid systems are remarkably higher than that of silica or nanoclay filled compounds. This can be explained by considering the partial break down of network structure of silica in NBR hybrid nanocomposites (NBR25:3 and NBR25:5). These results are in agreement with the silica-nanoclay dual structure, which is responsible for the synergistic effect observed in the DMTA results of hybrid samples.

Burst Stength

There is a mathematical formula that calculates the relationship of internal pressure (P) to allowable stress, nominal thickness, and diameter of the sphere. Simply stated, Barlow's formula calculates the pressure containing capabilities of a component[3]. The formula takes into account the sphere diameter (*D*), wall thickness (*t*), and the manufacturer's specified minimum yield strength of the component (*S*):

$$P = 4St / D \quad ...4$$

In elastomers, the component effective thickness depends on the material elongation capability. On the other hand, the effective wall thickness for elastomers continuously decreases as the component stretches under the internal pressure applied on the hemisphere. This phenomenon has been considered by a correction factor theoretically correlated with "elongation at break", namely λ. Finally; we will have

$$P = 400St / D\lambda \quad ...5$$

According to *Equation 5*, the ratio of tensile strength to elongation at break plays a key role in burst strength. As it can be seen in *Table 5*, hybrid compounds (NBR25:3 and NBR25:5) show higher burst strength compared to silica or nanoclay filled NBR compounds. It may be attributed to the synergistic effect between the silica and nanoclay in NBR matrix.

CONCLUSION

The effects of silica and nanoclay on mechanical and vulcanisation characteristics of the NBR compounds were investigated. The results of TEM show that the most of the

organoclay platelets are well dispersed in the NBR matrix, and intercalated microstructure formed in hybrid compounds. These results are consistent with the results obtained in WAXD patterns. The optimum cure time and scorch time both decrease with adding the silica to NBR compounds. This phenomenon can be explained by increases in the compound viscosity and thus the shear heating effect in the silica filled NBR compounds. Also, it may be due to the increase in effective filler volume by bound rubber for the silica. Considerable improvements in dynamic storage modulus and a steady decrease in tanδ values are observed in hybrid NBR compounds. This can be the consequence of good polymer–filler interaction. The deviation between theoretical and experimental values of storage modulus for hybrid samples can be explained on the basis silica-nanoclay dual structure formation between silica particles and nanoclay platelets in hybrid samples. Moreover, NBR samples containing a combination of silica and nanoclay show an increase in strength properties of the composites. This suggests a synergistic effect between the silica and nanoclay. This is in agreement with data generated by using Barlow's equation which calculates burst strength.

Date of receipt: August 2018
Date of acceptance: May 2018

REFERENCES

1. THOMAS, P.C., TOMLAL, J.E., SELVIN, T.P., SABU, T. AND JOSEPH, K. (2010) High-Performance Nanocomposites Based on Arcylonitrile-Butadiene Rubber With Fillers of Different Particle Size: Mechanical and Morphological Studies. *Polym. Composite*, **31(9)**, 1515 – 1524.

2. CHEN, S., YU, H., REN, W. AND ZHANG, Y. (2009) Thermal Degradation Behavior of Hydrogenated Nitrile-Butadiene Rubber (HNBR)/Clay Nanocomposite and HNBR/ Clay/Carbon Nanotubes Nanocomposites. *Thermochim. Acta*, **491(1-2)**, 103 – 108.

3. CHAYAN, D. AND BHARAT, K. (2012) Preparation and Studies of Nitrile Rubber Nanocomposites with Silane Modified Silica Nanoparticles. *Res. J. Rec. Sci.*, **1(2)**, 357 – 360.

4. DAVOODI, A.A., KHALKHALI, T., SALEHI, M.M. AND SARIOLETLAGH FARD, S. (2014) Burst Diaphragms Based on Carbon Black/Silica Hybrid Filler Reinforced Nitrile Rubber Compounds. *J. Soft Mater.*, **2014(article ID 498563)**, 1 – 8.

5. PRAVEEN, S., CHATTOPADHYAY, P.K., ALBERT, P. AND DALVI, V.G. (2009) Synergistic Effect Of Carbon Black And Nanoclay Fillers in Styrene Butadiene Rubber Matrix: Development of Dual Structure. *Compos. Part A-Appl. Sci.*, **40(3)**, 309 – 316.

6. ISMAIL, H. AND AHMAD, H.S. (2013) The Properties of Acrylonitrile-Butadiene Rubber (NBR) Composite with Halloysite Nanotubes (Hnts) and Silica or Carbon Black. *Polym. Plast. Technol. Eng.*, **52(12)**, 1175 – 1182.

7. PEREZ, L.D., ZULUAGA, M.A., KYU, T. AND MARK, J.E. (2009) Preparation, Characterization, and Physical Properties of Multiwall Carbon Nanotube/Elastomer Composites. *Polym. Eng. Sci.*, **49(5)**, 866 – 874.

8. HWANG, W.G., WEI, K.H. AND WU, C.M. (2004) Mechanical, Thermal, and Barrier Properties of NBR / Organo-Silicate Nanocomposites. *Polym. Eng. Sci.*, **44(11)**, 2117 – 2124.

9. LI, Q., ZHAO, S. AND PAN, Y. (2010) Structure, Morphology, and Properties of HNBR Filled with N550, SiO_2, ZDMA, and Two of Three Kinds of Fillers. *J. Appl. Polym. Sci.*, **117(1)**, 421 – 427.

10. OSTAD MOVAHED, S., ANSARIFAR, A. AND MIRZAIE, F. (2015) Effect of Various Efficient Vulcanization Cure Systems on the Compression Set of a Nitrile Rubber Filled with Different Fillers. *J. Appl. Polym. Sci.*, **132(8)**, 41512(1 – 10).

11. SOMBATSOMPOP, N., WIMOLMALA, E. AND SIRISINHA, C. (2008) Fly Ash Particles and Precipitated Silica as Fillers in Rubbers. III. Cure Characteristics and Mechanical and Oil-Resistance Properties of Acrylonitrile–Butadiene Rubber. *J. Appl. Polym. Sci.*, **110(5)**, 2877 – 2883.

12. HOSSEINI, S.M. AND RAZZAGHI-KASHANI, M. (2014) Vulcanization Kinetics of Nano-silica Filled Styrene Butadiene Rubber. *Polymer*, **55(24)**, 6426 – 6434.

13. BENDAHOU, A., KADDAMI, H., ESPUCHE, E. AND GOUANVÉ, F. (2011) Synergism Effect of Montmorillonite and Cellulose Whiskers on the Mechanical and Barrier Properties of Natural Rubber Composites. *Macromol. Mater. Eng.*, **296(8)**, 760 – 769.

14. SALKHORD, S., AND SADEGHI GHARI, H. (2015) Synergistic Reinforcement of NBR by Hybrid Filler System Including Organoclay and Nano-$CaCO_3$. *J. Appl. Polym. Sci.*, **131(44)**, 42744 – 42758.

15. YAN, H., SUN, K. AND ZHANG, Y. (2005) Effect of Nitrile Rubber on Properties of Silica-filled Natural Rubber Compounds. *Polym. Test.*, **24(1)**, 32 – 38.

16. ASTM D412-06a, Standard Test Methods for Vulcanized Rubber and Thermoplastic Rubbers and Thermoplastic Elastomers-Tension, ASTM International, West Conshohocken, PA, 2006.

17. ASTM D2240-05, Standard Test Method for Rubber Property—Durometer Hardness, ASTM International, West Conshohocken, PA, 2005.

18. ASTM E1640-09, Standard Test Method for Assignment of the Glass Transition Temperature By Dynamic Mechanical Analysis, ASTM International, West Conshohocken, PA, 2009.

19. SOUSA, D.B.F., MANTOVANI, G.L. AND SCURACCHIO, C.H. (2011) Mechanical Properties and Morphology of NBR with Different Clays. *Polym. Test.*, **30(8)**, 819 – 825.

20. SENGUPTA, R., CHAKRABORTY, S., BANDYOPADHYAY, S. AND DASGUPTA, S. (2007) A Short Review on Rubber/Clay Nanocomposites with Emphasis on Mechanical Properties. *Polym. Eng. Sci.*, **47(11)**, 1956 – 1974.

21. WANG, M.J., WOLFF, S. AND DONNET, J.B. (1991) Filler-Elastomer Interactions. Part I. Silica Surface Energies and Interactions with Model Compounds. *Rubber Chem. Technol.*, **64(4)**, 559 – 576.

22. NAH, C., RYU, H.J., KIM, W.D. AND CHANG, Y.W. (2003) Preparation and Properties of Acrylonitrile–Butadiene Copolymer Hybrid Nanocomposites with Organoclays. *Polym. Int.*, **52(8)**, 1359 – 1364.

23. CHOI, S.S., PARK, B.H. AND SONG, H. (2004) Influence of Filler Type and Content on Properties of Styrene-Butadiene Rubber (SBR) Compound Reinforced with Carbon Black or Silica. *Polym. Adv. Tech.*, **15(3)**, 122 – 127.

24. LEE, J., HONG, J., PARK, D.W. AND SHIM, S.E. (2009) Production of Carbon Black/ Silica Composite Particles by Adsorption of Poly(vinyl pyrrolidone). *Macromol. Res.*, **17(9)**, 718 – 720.

25. RATTANASOM, N., SAOWAPARK, T. AND DEEPRASERTKUL, C. (2007) Reinforcement of Natural Rubber with Silica/Carbon Black Hybrid Filler. *Polym. Test.*, **26(3)**, 369 – 377.

26. GUTH, E. AND GOLD, O. (1938) Hydrodynamical Theory of the Viscosity of Suspension. *Phys. Rev.*, **53(1)**, 322 – 328.

27. WU, Y.P., JIA, Q.X., YU, D.S. AND ZHANG, L.Q. (2004) Modeling Young's Modulus of Rubber–Clay Nanocomposites Using Composite Theories. *Polym. Test.*, **23(8)**, 903 – 909.

28. GUTH, E. AND GOLD, O. (1938) Hydrodynamical Theory of the Viscosity of Suspension. *Phys. Rev.*, **53(1)**, 322 – 328.

29. WU, Y.P., JIA, Q.X., YU, D.S. AND ZHANG, L.Q. (2004) Modeling Young's Modulus of Rubber–Clay Nanocomposites Using Composite Theories. *Polym. Test.*, **23(8)**, 903 – 909.

30. NORIMAN, N.Z. AND ISMAIL, H. (2013) Effect of Carbon Black/Silica Hybrid Filler on Thermal Properties, Fatigue Life, and Natural Weathering of SBR/recycled NBR Blends. *Int. J. Polym. Mater. Polym. Bio-Mater.*, **62(5)**, 252 – 259.